ELSEVIER

Thermochimica Acta 379 (2001) 241–254

thermochimica acta

www.elsevier.com/locate/tca

H_2S adsorption on a sulfided $CoMo/Al_2O_3$ catalyst under flow and pressure conditions: a thermodynamic and modelization study

Michaël Echard, Jacques Leglise*

Laboratoire Catalyse et Spectrochimie, Université de Caen ISMRA, UMR CNRS 6506, 6 Boulevard du Maréchal Juin, ISMRA, F-14050 Caen, France

Abstract

The amount of H_2S adsorbed on a sulfided $CoMo/Al_2O_3$ hydrotreating catalyst has been measured under flow conditions using a high pressure thermogravimetric technique. The measurements have been performed under a wide range of conditions: at 313–573 K with a mixture of H_2S and CH_4 (0.015–0.35 MPa) obtained from the decomposition of dimethyldisulfide diluted in H_2 (1.8–3.8 MPa). Five isotherms determined at temperatures below, near, and above the critical temperature of H_2S, were established from isobaric measurements. The adsorbed phase was found to consist essentially of H_2S. The thermodynamics of H_2S sorption was studied in order to obtain information about the state of the adsorbed phase and the mutual interaction between adsorbed H_2S molecules or dissociated H_2S species, and about the homogeneity or the heterogeneity of the catalyst surface. The experimental isotherms were compared to 15 isotherm models featuring mobile adsorption and localized molecular or dissociative adsorption on a single-, two- and multi-site surface. Discrimination among rival models was based on statistics and theory. Two models were retained: the generalized Freundlich model featuring adsorption of H_2S molecules on a patch-wise distribution of sites, and the Langmuir model characterized by the dissociative chemisorption of H_2S on dual-sites on both CoMo sulfide phases and alumina. Using the latter model, the amount of adsorbed H_2S on the supported CoMo sulfide phases was determined under conditions close to industrial practice.

Keywords: Hydrotreating catalyst; H_2S adsorption; Adsorption under pressure and flow conditions; Thermogravimetric analysis; Isotherm modeling

1. Introduction

Most of the studies on gas or liquid adsorption at high pressures [1–3] are devoted to the determination of the adsorption properties of adsorbents such as carbon or zeolite for the purpose of multi-component separation processes [4]. Conditions are often restricted to low temperature, e.g. under the critical temperature of the products that need to be separated. Moreover, studies are rarely performed in a flowing mode, although most of the industrial processes for gas–liquid separation or catalysis are operated under flow conditions. In addition, rate equations based on Langmuir–Hinshelwood formalism [5] include an inhibition term due to the competitive adsorption of reactants, inhibitors and poisons, which makes difficult the determination of kinetic parameters. For instance, in the case of hydrotreatment processes that are intended to produce cleaner fuels, the catalyst activity for gas–oil desulfurization is strongly inhibited by the produced H_2S [6]. Thus, knowing how and how much H_2S adsorbed on the working catalyst should be useful for improving the catalyst performance.

* Corresponding author. Fax: +33-2-31-45-28-22.
E-mail address: leglise@imsra.fr (J. Leglise).

0040-6031/01/$ – see front matter
PII: S0040-6031(01)00622-0

The aim of this work is, therefore, to evaluate the adsorption properties with respect to H_2S of a typical hydrotreating $CoMo/Al_2O_3$ catalyst under conditions relevant to catalysis. Due to the low reactivity of the refractory sulfur aromatic compounds present in oils, catalysts are operated under a stream of hydrogen at high pressure (3–4 MPa) and high temperature (573–653 K) [6]. Under these conditions, the Co and Mo oxides supported on the inert γ-alumina are converted into stable Co_9S_8 and MoS_2 sulfides, or mixed Co–Mo–S particles in which Co atoms decorate the edges of MoS_2 slabs [7]. These metal sulfide phases are the active catalysts.

According to the literature, H_2S adsorbs either molecularly or dissociatively on the catalytic sites [8–10]. Sulfhydric SH active species [11–13] have been evidenced by spectroscopic methods on the CoMo sulfide phases [14,15]. In addition, H_2S adsorbs either on exposed Lewis Al^{3+} sites or via hydrogen bonding to the hydroxyl groups of the alumina support [8,9].

The eventual presence of multiple H_2S species and the heterogeneity of the catalyst surface highlight the need for a detailed investigation of the H_2S adsorption phenomenon.

This study focuses on the determination of the adsorption properties of a sulfided $CoMo/Al_2O_3$ catalyst. Measurements were performed at temperatures ranging from 313 to 573 K under pressure and flow conditions. The H_2S uptake has been determined by in situ thermogravimetry and gas analyses, using various partial pressures of H_2S. The experimental isotherms are compared to theoretical models featuring mobile and localized adsorption on a homogeneous or heterogeneous surface. The thermodynamics of H_2S adsorption is studied.

2. Experimental

2.1. Gravimetric pressure apparatus

Gravimetric measurements were performed in a high pressure adsorption chamber coupled to an analytical balance (Fig. 1) by means of a suspension magnetic device from Rubotherm. Basically, the device consists of an CoSm permanent magnet that is placed in a thermosated pressurized housing above the reactor, and of an electromagnet hooked on the pan of the analytical balance [16]. The permanent magnet

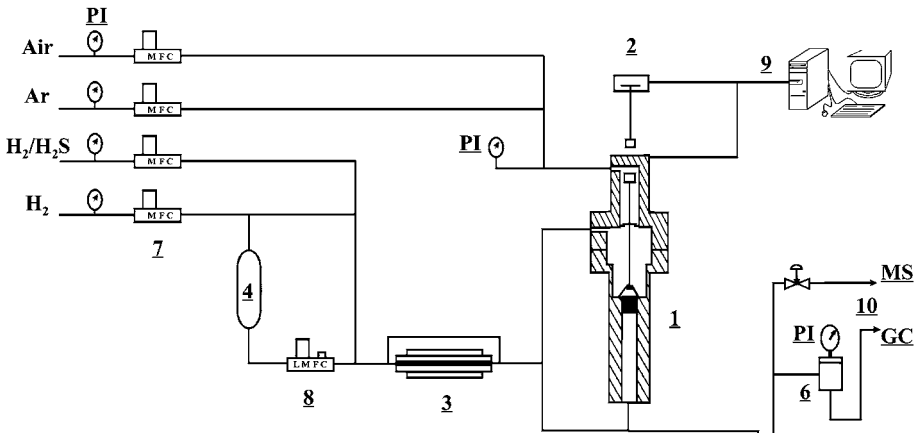

Fig. 1. Schematic view of the experimental setup and flow diagram.

is fixed on top of a stainless steel vertical rod, and the adsorbent solid was placed in a 7 cm^3 basket coupled to the bottom of the rod by means of a steel cone and tripod part [17].

In the zero point position, the basket load is decoupled from the permanent magnet; the upper part of the basket sits on the reactor internal wall. With such reactor design, the gases flow through the adsorbent bed, allowing measurements under plug-flow and high pressure conditions similar to those used in hydrotreating processes.

2.2. Mass determination

In the measurement position, the permanent magnet is lifted up and it becomes coupled to the basket load [17]. Three measurements were recorded every 2 min after a 20 s stabilization period in the suspended state. The mass was found to be identical to that obtained at steady-state after isolating the adsorption chamber, so that convection and thermomolecular effects [18] were negligible. The differences between the masses recorded in the zero-point and measurement positions gave the mass m_e of the basket and tripod parts together with those of the adsorbent solid and adsorbed phase. The variation in mass δm due to adsorption was corrected for buoyancy as follows:

$$\delta m = [m_e + \rho(V_a + V_b + V_c)] - [m^0 + \rho^0(V_a + V_b + V_c)] \quad (1)$$

where ρ is the gas phase density at T and P under investigation; ρ^0, the density of the reference state (air, 1.1849 g cm^{-3}); m^0, the mass of the basket-tripod part (12.262 g) and adsorbent (typically 3.6 g); V_b, and V_c the volumes of the basket-tripod part and catalyst, respectively. The correction due to the volume of the adsorbed phase V_a could be neglected, in agreement with de Weireld et al. [17]. From three replicate experiments with a fresh catalyst, the relative errors on the adsorbed mass were estimated to be less than 5%.

2.3. Materials

Hydrogen, H_2S (5 mol%)–H_2, argon, and helium gases are from Air Liquide (Grade U), and air is atmospheric. All gases, excepting H_2 and the H_2S–H_2 mixture, were dried on zeolite traps before use. The adsorbent solid is a commercial hydrotreating $CoMo/Al_2O_3$ catalyst (HR306C, 2.4 wt.% Co and 9.3% Mo) from Procatalyse. Its specific volume was 0.258 $cm^3\ g^{-1}$. From N_2 sorption at 77 K, the specific surface area was 200 $m^2\ g^{-1}$ and the mesoporous volume 0.53 $cm^3\ g^{-1}$.

2.4. $CoMo/Al_2O_3$ sulfidation

The $CoMo/Al_2O_3$ sample (3.6 g, grains 0.2–0.5 mm) was sulfided in the pressure chamber (Fig. 1) before carrying out the adsorption measurement. The catalyst sample was first calcined under air (3.6 l h^{-1}) at 673 K. The system was flushed with Ar at 313 K and pressurized with hydrogen at 3.8 MPa. The adsorption chamber was then by-passed, and a flow of H_2, H_2S and CH_4 was established. H_2S and CH_4 were produced in equal amounts by complete conversion of dimethyldisulfide (DMDS) at 623 K under the H_2 flow (5 l h^{-1}) in a pre-reactor loaded with 100 g of a sulfided $CoMo/Al_2O_3$ catalyst. The DMDS and H_2 feed rates were regulated using mass flow controllers, so that the partial pressures of H_2 and H_2S could be varied independently. The partial pressure of H_2S (and CH_4) was controlled by gas chromatography.

Once, the partial pressure of H_2S has been set to 0.2 MPa, the sulfiding gas was introduced in the adsorption chamber. The solid was stabilized for 5 h under flow before heating to 673 K (ramp 180 K h^{-1}) for 8 h. The catalyst was cooled and removed under Ar in order to determine the sulfur content. Chemical analysis yielded 7.37 ± 0.2 wt.% of sulfur, similar to the stoichiometric amount (7.45 wt.%) expected for complete sulfidation into Co_9S_8 and MoS_2. Therefore, the adsorption measurements were performed on a totally sulfided catalyst.

2.5. Adsorption measurement

At the end of the sulfidation stage, the catalyst was cooled down to 313 K under the flowing gas mixture. The catalyst was then heated up to 573 K with intermediate steps lasting for 6 h at 353, 403, and 493 K. The cooling/heating sequence was repeated using another partial pressure of H_2S in the range 0.015–0.35 MPa. Thus, adsorption measurements

were obtained when the catalyst was cooled down, and desorption measurements when the catalyst was heated. Five isotherms at 313, 353, 403, 493, and 573 K were obtained from isobaric measurements. Three temperature domains were investigated according to the H_2S critical temperature ($T_c = 373.2$ K) [19]: (1) the subcritical region at 313–353 K; (2) near T_c at 353–403 K; and (3) the supercritical region at 403–573 K. The measurement at 573 K was relevant to hydrotreating catalysis conditions [6]. Measurements were not performed at temperatures higher than 623 K because of a slow continuous corrosion of the steel basket by H_2S.

The influence of H_2 has been assessed using 1.8 MPa instead of 3.8 MPa H_2 pressure, and that of CH_4 by switching the H_2S–CH_4–H_2 gas mixture to H_2S–H_2, while keeping constant H_2S and H_2 pressures at 0.2 and 3.8 MPa, respectively.

2.6. Adsorption models

Fifteen adsorption models featuring localized and mobile adsorption on a homogeneous or heterogeneous surface were tested. The model names and the isotherm equations are gathered in Table 1 with the parameters under study. The adsorption parameters were estimated by a non-linear regression technique after minimizing the maximum likelihood objective function with respect to the mass residuals at each temperature set. The adequacy of the model was indicated by the sum of squares of the residuals SSE, by the correlation coefficient R^2, and after graphical inspection. The significance of the overall regression was tested by calculation of F statistics.

3. Results and discussion

3.1. $CoMo/Al_2O_3$ sulfidation

Fig. 2 shows the mass variation recorded during the in situ sulfidation of the oxidic $CoMo/Al_2O_3$. When the sulfiding H_2S–CH_4–H_2 gas mixture contacted the catalyst at 313 K, the mass increased by 7.7% compared to the mass of the oxidic sample. The mass increase was due to adsorption of H_2S species and to a partial sulfidation of the Co and Mo oxides [24]. Upon raising the temperature, the mass decreased in two stages, rapidly until 413 K, then at a slower rate up to 573 K. From gas phase analyses, this was interpreted by the opposite effects between sulfidation of the Co and Mo oxides and desorption of the excess H_2S and the produced H_2O [24]. Then, the mass increased slightly during the isothermal stage at 673 K, because of the removal of the water formed by heavier H_2S molecules.

The final increase in mass at 673 K was found to be 4.8% compared to the mass of the dry oxidic catalyst, a higher value than the 2.1% increase due to the exchange of CoMo metal oxygen by sulfur atoms. Thus, the 2.7% excess mass was due to molecular or dissociated H_2, CH_4 and H_2S species adsorbed on the $CoMo/Al_2O_3$ surface.

3.2. Adsorption and desorption measurements

After the sulfidation stage at 673 K, the temperature was decreased to 313 K. As a result, the mass regularly increased (Fig. 2). The catalyst was in a steady-state in less than 20 min at 313 K, showing that equilibrium between the gas and the adsorbed phase was relatively fast under flow and pressure conditions. The solid gained 0.085 g per gram of the oxidic precursor (Fig. 2), but only 0.063 g compared to the mass of the sulfided catalyst. The adsorbed masses on the sulfided catalyst collected at the intermediate temperatures 353–493 K are listed in Table 2. Interestingly, the results shows that the catalyst was essentially in steady-state since the mass gains measured during the decrease in temperature were similar to those measured after a stepwise increase in temperature (Table 2). Furthermore, it implies that capillary condensation did not occur under these pressure conditions.

3.3. Nature of the adsorbed phase

We first established, what gas (H_2, CH_4, or H_2S) was preferentially adsorbed. As shown in Table 2, the adsorbed masses were similar when the hydrogen pressure was decreased from 3.8 to 1.8 MPa, while keeping constant both CH_4 and H_2S partial pressures. Thus, the mass of adsorbed hydrogen was negligible compared to that of CH_4 and H_2S.

On the other hand, the mass gains measured in presence of CH_4 were similar to those measured without CH_4 (Table 2). Therefore, it can be inferred

Table 1
Adsorption models for localized or mobile adsorption on a homogeneous or heterogeneous surface

Name	Description	Reference	Equation[a]	Parameters
Mobile adsorption				
Vo	Volmer	[20]	$\theta = \frac{KP\exp(-\theta/1-\theta)}{1+KP\exp(-\theta/1-\theta)}$	m_∞, K
Hi	Hill with adsorbate–adsorbate interaction	[20]	$\theta = \frac{KP\exp(-\theta/(1-\theta)+\alpha\theta)}{1+KP\exp(-\theta/(1-\theta)+\alpha\theta)}$	m_∞, K, α
Localized adsorption, single site				
L1m	Langmuir, molecular adsorption	[5]	$\theta = \frac{KP}{1+KP}$	m_∞, K
FG	Fowler–Guggenheim, molecular adsorption with adsorbate–adsorbate interaction	[20]	$\theta = \frac{KP\exp(\omega\theta)}{1+KP\exp(\omega\theta)}$	m_∞, K, ω
L1d	Langmuir, dissociative adsorption	[5]	$\theta = \frac{\sqrt{KP}}{1+\sqrt{KP}}$	m_∞, K
Localized adsorption, two sites[b]				
L2m	Langmuir, molecular adsorption	–	$\theta = \frac{(1-f)K_AP}{1+K_AP} + \frac{fK_MP}{1+K_MP}$	m_∞, f, K_A, K_M
L2sm	Simplified L2m model	–	$\theta = \frac{(1-f)K_AP}{1+K_AP} + f$	m_∞, f, K_A
L2d	Langmuir, dissociative adsorption	–	$\theta = \frac{(1-f)\sqrt{K_AP}}{1+\sqrt{K_AP}} + \frac{f\sqrt{K_MP}}{1+\sqrt{K_MP}}$	m_∞, f, K_A, K_M
L2sd	Simplified L2d model	–	$\theta = \frac{(1-f)\sqrt{K_AP}}{1+\sqrt{K_AP}} + f$	m_∞, f, K_A
Multi-site adsorption				
GL	Generalised model, molecular adsorption	[21]	$\theta = \left[\frac{(KP)^n}{1+(KP)^n}\right]^{t/n}$	m_∞, K, t, n
FL	Freundlich generalised, molecular adsorption	[22]	$\theta = \left[\frac{KP}{1+KP}\right]^t$	m_∞, K, t
To	Toth, molecular adsorption	[23]	$\theta = \left[\frac{(KP)^n}{1+(KP)^n}\right]^{1/n}$	m_∞, K, n
Si	Sips, molecular adsorption	[5]	$\theta = \frac{(KP)^n}{1+(KP)^n}$	m_∞, K, n
Fr	Freundlich, molecular adsorption	[5]	$\theta = (KP)^t$	m_∞, K, t
Te	Temkin, molecular adsorption	[5]	$\theta = \frac{1}{\gamma}\ln(KP)$	m_∞, γ, K

[a] Fractional uptake θ expressed as $\delta m/m_\infty$ with δm the adsorbed H_2S mass and m_∞ the mass at saturation, mass in g g_s^{-1}.
[b] A and M stand for alumina and CoMo sulfides, respectively.

that CH_4 was weakly adsorbed compared to H_2S. Such finding is supported by binary adsorption studies of light alkanes and H_2S. H_2S was reported to be more adsorbed than CH_4 on a homogeneous carbon adsorbent at 298 K [16], and more than propane on a heterogeneous protonated mordenite HM at 283–363 K [25].

In conclusion, one can ascertain that the excess mass corresponds essentially to H_2S molecules or dissociated species adsorbed on the sulfided CoMo/Al_2O_3 catalyst.

3.4. H_2S adsorption isotherms

The five isotherms are shown in Fig. 3. The shape of the isotherms agrees with the type I isotherms according to the IUPAC classification. No hysteresis was observed between adsorption and desorption steps so that the isotherms were perfectly reversible in the investigated pressure range.

The results showed that the catalyst surface was readily saturated at low H_2S pressure. At 313 K, the mass of H_2S adsorbed at 0.015 MPa H_2S partial

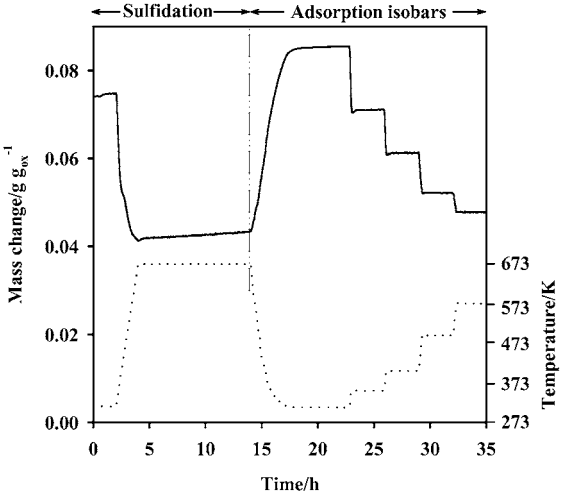

Fig. 2. Catalyst mass change per gram of oxidic $CoMo/Al_2O_3$ during the sulfidation stage at 673 K and the first isobaric adsorption measurement at $P_{H_2S} = P_{CH_4} = 0.19$ MPa, $P_{H_2} = 3.8$ MPa. Temperature right scale.

pressure represented more than 50% of the mass adsorbed at the highest investigated pressure of 0.35 MPa. This proportion increased drastically with the temperature of adsorption. Therefore, the results suggest that H_2S is strongly adsorbed on the catalyst surface, presumably on both sulfided CoMo and alumina sites.

The H_2S uptakes were found to be 4–5 times higher on the sulfided $CoMo/Al_2O_3$ catalyst than those reported at 298–423 K on γ-aluminas of comparable specific surface area under similar H_2S partial pressures [8,10]. Thus, the $CoMo/Al_2O_3$ catalyst has certainly a higher site density than γ-alumina, which is certainly due to the presence of the CoMo sulfides on the alumina support. This is further corroborated by comparing the adsorption data with those obtained under comparable conditions on larger area adsorbents: zeolite HM [25] and carbon [16,26]. Per unit surface area, the amount of H_2S adsorbed on $CoMo/Al_2O_3$ was found to be 2–3 times higher than those measured on zeolite HM and carbon. One can indeed expect a higher affinity of H_2S with the sulfided CoMo phases than with the surface of the non-polar carbon or the heterogeneous silico–aluminate HM. In conclusion, the above comparisons suggest that H_2S would adsorb more on the sulfided CoMo phases than on the exposed alumina surface of the $CoMo/Al_2O_3$ catalyst.

3.5. Thermodynamics of H_2S adsorption

The energetics of sorption was studied to know about the adsorption mode of H_2S and the mutual interaction between adsorbed molecules. The isosteric heat of adsorption Q_{st} was calculated at constant adsorbed mass. The classical Clausius–Clapeyron relationship [27] applies, because the investigated H_2S partial pressures were far below the critical pressure of H_2S (8.9 MPa [19]). Fig. 4 shows the variation of Q_{st} calculated every 0.0005 g within the experimental mass range; the equilibrium pressures were determined by fitting the experimental isotherms using model L2sd (Table 1).

Interestingly, Q_{st} appears to be dependent on temperature (Fig. 4). In the subcritical domain, 313–353 K, Q_{st} was found to be constant and low,

Table 2
Influence of experimental conditions[a] on the adsorbed mass per gram of sulfided $CoMo/Al_2O_3$ catalyst

	Adsorbed mass (g g_s^{-1})			
Mode	Adsorption	Desorption	Desorption	Desorption
Compounds	H_2, H_2S=CH_4	H_2, H_2S=CH_4	H_2, H_2S=CH_4	H_2, H_2S
P (MPa)	3.8, 0.189	3.8, 0.189	1.8, 0.184	3.8, 0.191
T (K)				
313	0.0627	0.0622	0.0649	–
353	0.0486	0.0490	0.0503	0.0488
403	0.0389	0.0394	0.0398	0.0387
493	0.0301	0.0305	0.0306	0.0321
573	0.0250	0.0262	0.0266	0.0284

[a] Adsorption: ramping lower than 5 K min^{-1}; desorption: step-wise increasing temperature.

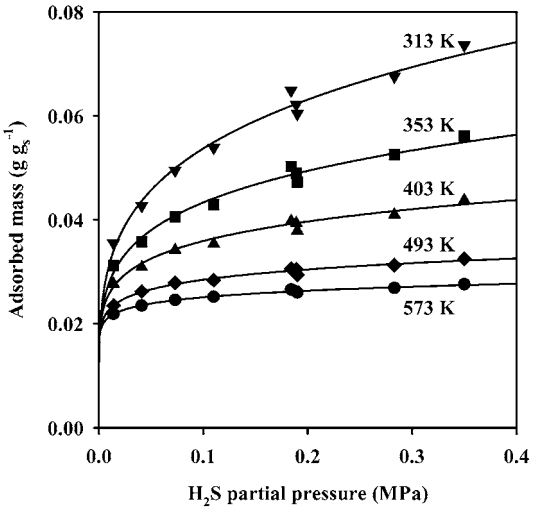

Fig. 3. H_2S adsorption isotherms on the sulfided $CoMo/Al_2O_3$ catalyst.

approaching the heat of H_2S liquefaction (L_{H_2S} = 14 kJ mol^{-1} [28]). Thus, H_2S does not seem to interact strongly with the catalyst surface, suggesting that the adsorbed phase was in a mobile state below T_c. Such behavior was also found in the critical domain, 353–403 K. In the supercritical domain, 403–573 K, the Q_{st} values were much higher and increased with coverage, suggesting that the adsorbed phase became more localized. This apparently contradicts the common observation that an adsorbed phase gains in mobility with increasing temperature [29].

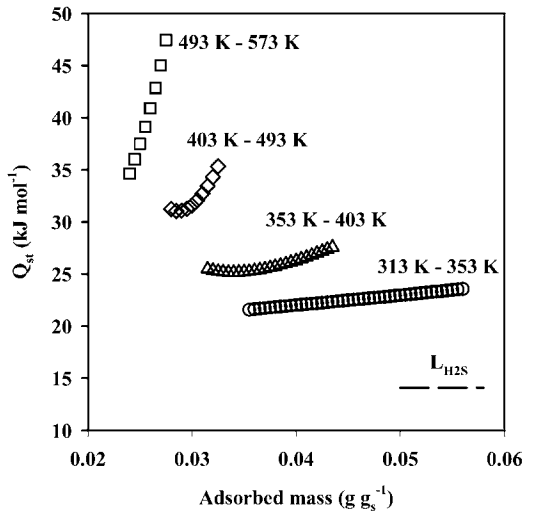

Fig. 4. Variation of the isosteric heat Q_{st} with the mass of adsorbed H_2S on the sulfided $CoMo/Al_2O_3$ catalyst. Dashed line: L_{H_2S}, heat of H_2S liquefaction at 298 K.

Several explanations can account for the observed low values and variation of Q_{st}. Firstly, localized adsorption can be almost identical with mobile adsorption when the catalyst pores are much larger than the size of the adsorbed molecule [29]. This is the case here, since the average pore radius was 5 nm and the H_2S radius 0.362 nm [19]. On the other hand, the variation of Q_{st} can be caused by interactions between neighboring adsorbed H_2S molecules. Indeed, much higher Q_{st} values (>130 kJ mol^{-1}) were reported at zero coverage on γ-alumina [8]. In this work [8], Q_{st} decreased rapidly to a low value and stayed constant beyond the very low H_2S uptake of 0.002 g g^{-1}. This resembles what was found here with $CoMo/Al_2O_3$ near and below T_c (Fig. 4). In the supercritical temperature domain (493–573 K), the catalyst seemed to be saturated at low H_2S partial pressure. Thus, lateral interactions are likely, causing an increase in Q_{st} with coverage, as reported by Gachet and Trambouze [27] in their study of N_2 sorption on alumina under supercritical conditions.

The properties regarding the mobility of the adsorbed H_2S phase was thus examined by studying the variation in entropy with the H_2S uptake. The differential entropy of adsorption $\Delta\dot{S}_a$ was calculated at a given experimental temperature and reference pressure P° set at 0.1 MPa is as follows:

$$\Delta\dot{S}_a = \dot{S}_a - S_g^\circ = -\frac{Q_{st}}{T} + R\ln\left(\frac{P^\circ}{P}\right) \quad (2)$$

The variations in entropy $\Delta\dot{S}_a$ are shown in Fig. 5. Note that, $\Delta\dot{S}_a$ was found to be independent of the temperature in a particular domain of mass where Q_{st} was temperature invariant; the two terms on the right side of Eq. (2) compensating each other. Table 3 shows that $\Delta\dot{S}_a$ decreased with the H_2S uptake, from −53 to −77 J mol^{-1} K^{-1} at 313–353 K and slightly more from −56 to −93 J mol^{-1} K^{-1} at the highest temperatures.

The observed variations were then compared to the expected changes in entropy due to localized or mobile adsorption. Upon adsorption, the H_2S gas molecule looses its translational entropy $\dot{S}_{tr}$ and part of the rotational entropy $\dot{S}_R$. For the mobile case, the sorbed phase will however gain a translational term

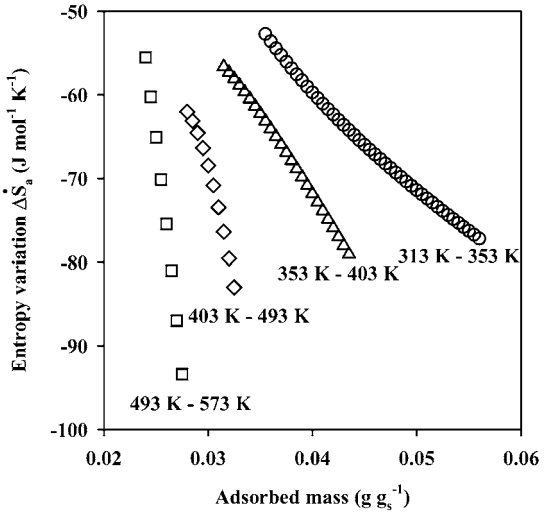

Fig. 5. Variation of the adsorption entropy $\Delta\dot{S}_a$ with the mass of adsorbed H_2S on the sulfided $CoMo/Al_2O_3$ catalyst.

due to the motion of H_2S in directions parallel to the surface [5], which can be conveniently separated into a molecular term $\dot{S}_{m,tr}$ and a configurational term $\dot{S}_{m,\theta}$ depending on the fraction θ of the intracrystalline volume occupied by H_2S. The molecular term $\dot{S}_{m,tr}$ was determined assuming that H_2S molecules were arranged in a hexagonal close-packing liquid-like phase. For the localized case, the adsorption entropy will gain a configurational term $S_{1,\theta}$ due to the number of ways to distribute H_2S molecules on the surface [5].

Hence, the expected changes in entropy caused by the loss of thermal translation and rotation for localized and mobile adsorption are respectively:

$$\Delta\dot{S}_l = -\left(\dot{S}_{tr} - \frac{n}{3}\dot{S}_R\right) \text{ and} \quad (3)$$

$$\Delta\dot{S}_m = -\left(\dot{S}_{tr} - \frac{n}{3}\dot{S}_R\right) + \dot{S}_{m,tr} \quad (4)$$

These changes in entropy are listed in Table 3 for two typical cases, i.e. with 0 and 2 lost degrees of rotational freedom. Therefore, the difference between $\Delta\dot{S}_a$ and the entropy change due to translation and rotation $\Delta\dot{S}_l$ or $\Delta\dot{S}_m$ is equal to the change in vibrational and configurational entropies.

$$\Delta\dot{S}_a - \Delta\dot{S}_l = \Delta\dot{S}_{l,v} + \dot{S}_{l,\theta} \quad (5)$$

$$\Delta\dot{S}_a - \Delta\dot{S}_m = \Delta\dot{S}_{m,v} + \dot{S}_{m,\theta} \quad (6)$$

From Table 3, the differences $\Delta\dot{S}_a - \Delta\dot{S}_l$ and $\Delta\dot{S}_a - \Delta\dot{S}_m$ are in all cases positive in sign. They were related to the theoretical variation of the vibrational and configurational terms. Both configurational terms decrease with the H_2S uptake, being nil at half coverage for localized adsorption and at $\theta = 0.36$ for mobile adsorption [29]. Since the fractional uptakes θ were greater than 0.4 at all temperatures and studied H_2S pressures, the configurational entropic terms, $\dot{S}_{l,\theta}$ and $\dot{S}_{m,\theta}$, are mainly negative in sign. Thus, the differences between the adsorption entropy $\Delta\dot{S}_a$ and the rotation and translation entropy loss was primarily due to a change in vibrational entropy.

$\Delta\dot{S}_a - \Delta\dot{S}_l$ for localized adsorption at the lowest uptakes was found to be about 100 J mol^{-1} K^{-1} without loss of rotational freedom (Table 3), and $\Delta\dot{S}_a - \Delta\dot{S}_m$ for mobile adsorption about 40 J mol^{-1} K^{-1}. The differences in entropy did not vary much with the

Table 3
Comparison of the experimental changes in differential entropy $\Delta\dot{S}_a$ calculated at constant mass (δm) of adsorbed H_2S (g g$_s^{-1}$) and the theoretical changes due to the loss of translational and rotational entropies upon localized $\Delta\dot{S}_l$ or mobile $\Delta\dot{S}_m$ adsorption (values in J mol^{-1} K^{-1})

	DOF[a]	Temperature (K)			
		333	378	448	533
$\Delta\dot{S}_a$		−53 to −77	−57 to −79	−62 to −83	−56 to −93
δm range		0.024 to 0.027	0.028 to 0.032	0.031 to 0.043	0.035 to 0.056
$\Delta\dot{S}_l$	0	−155	−158	−161	−165
	2	−191	−195	−200	−205
$\Delta\dot{S}_m$	0	−93	−94	−96	−97
	2	−128	−131	−134	−137

[a] DOF: degree of rotational freedom lost upon H_2S adsorption.

adsorption temperature, indicating that the nature of the H_2S adsorbed species was similar in the whole temperature range examined.

Stretching S–H vibration at 2500 cm^{-1} and bending H–S–H vibration at 1340 cm^{-1} [9,15] cannot account for such high entropic values. Metal–S or Al–S vibration frequencies are unfortunately not available, but they could compare to the 140–150 cm^{-1} values reported for metal–H and Al–H vibrations on MoS_2/Al_2O_3 [30]. With such low frequencies, the vibration entropies equaled to 12–17 J mol^{-1} K^{-1} at 313–573 K. The total vibration entropy should be much higher, e.g. Agarwal et al. [31] reported vibration entropy of about 70 J mol^{-1} K^{-1} for a variety of molecules adsorbed on carbon. Therefore, the vibrational entropy term is certainly higher than that expected for mobile adsorption.

Summarizing the thermodynamic study, it can be inferred that H_2S adsorbs locally on the surface of the $CoMo/Al_2O_3$ catalyst regardless of temperature. The increase of Q_{st} with H_2S coverage suggests an exothermic repulsion between adsorbed H_2S species or the occurrence of H_2S dissociation.

3.6. Modeling of adsorption isotherms

Several theoretical adsorption isotherms can be suitable for representing the experimental data. From the thermodynamic study, models featuring localized adsorption should be preferred. As a matter of fact, chemisorption predominates below and above T_c, since H_2S slowly desorbed at 313 or 573 K after 24 h under pure hydrogen flow, in agreement with a previous report on Al_2O_3 [9]. Multilayer adsorption models were not examined, because the investigated H_2S partial pressures were much lower than the saturation pressure (e.g. $P_{sat} = 2.86$ MPa at 303 K [19]), and because saturation was apparently attained above T_c at the highest studied H_2S partial pressure. Thus, Langmuir-type models that assume a monolayer of adsorbed H_2S molecules or dissociated species on a plane surface were tested. They were nevertheless compared with two models featuring mobile adsorption. The models studied are listed in Table 1; they are classified in four groups according to the mode of H_2S adsorption and the number of different types of adsorption sites.

Depending on the model, two to four parameters (Table 1) are required to fit the experimental data. The mass m_∞ of H_2S adsorbed at the monolayer can be estimated in all models, excepting in the Temkin model, where it cannot be distinguished from parameter γ [5]. The fraction f of the mass adsorbed on the supported CoMo sulfides is obtained with models L2m or L2d and their simplified forms L2sm or L2sd. Parameters K, K_M and K_A are Henry's law adsorption constants. Parameters α and ω are the interaction parameters for mobile and localized adsorption, respectively [5,20].

3.6.1. Regression results

The results of the regressions were examined first for the measurement at 313 K (Table 4). The F values were in all cases greater than tabulated F statistics, so that all models were apparently adequate. The better fits were obtained with the L2 models. It appears to be impossible to distinguish based on statistics the molecular adsorption models L2m and L2sm from the dissociated adsorption models L2d and L2sd. The fit was not improved by considering multi-site adsorption (4th group models). Modeling mobile adsorption using the Hill equation seemed satisfactory, contrarily to that using the Volmer equation. Finally, the Langmuir L1m and Fowler–Guggenheim models featuring molecular adsorption on a unique set of site had a poor predicting character ($R^2 < 0.90$). This was further supported by the graphical inspection in Fig. 6; models Vo, FG and L1m should be obviously discarded because the mass residuals were not randomly distributed.

The excellent fit obtained with the L2 models (Fig. 6b) indicates that the surface may comprise two major types of adsorption sites, most probably the CoMo sulfide phases and the exposed alumina. However, numerous sites do exist on the catalyst surface: the alumina sites and the various exposed metal atoms with different sulfur environments (zero to four sulfur vacancies) and local configurations (corner and edge sites) of Co-promoted MoS_2 crystallites [7]. This presumes a broad distribution of adsorption sites. Unfortunately, the modeling does not allow discriminating among the dual-site and multi-site models.

The above conclusions hold at higher temperatures (353–573 K). The quality of the fit was generally improved as shown in Table 4 for the measurement at 573 K. It was noteworthy that the models ranked

Table 4
Modeling regression results of the experimental data at 313 and 573 K — sum of squares of the residuals SSE, correlation coefficient R^2, and F statistic

Model	Number of parameters	313 K			573 K		
		SSE	R^2	F^a	SSE	R^2	F^a
Vo	2	11.3×10^{-5}	0.9064	68	12.6×10^{-7}	0.9526	141
Hi	3	4.13×10^{-5}	0.9707	99	2.75×10^{-7}	0.9931	431
L1m	2	19.2×10^{-5}	0.8347	35	45.4×10^{-7}	0.8198	32
FG	3	14.1×10^{-5}	0.8936	25	27.7×10^{-7}	0.8859	23
L1d	2	5.37×10^{-5}	0.9590	164	14.6×10^{-7}	0.9447	120
L2m	4	1.69×10^{-5}	0.9936	260	2.17×10^{-7}	0.9954	364
L2sm	3	1.76×10^{-5}	0.9928	411	3.09×10^{-7}	0.9926	400
L2d	4	4.79×10^{-5}	0.9664	48	11.9×10^{-7}	0.9570	37
L2sd	3	1.67×10^{-5}	0.9941	508	2.13×10^{-7}	0.9956	680
GL	4	2.21×10^{-5}	0.9885	143	2.15×10^{-7}	0.9955	371
FL	3	2.21×10^{-5}	0.9885	258	2.15×10^{-7}	0.9955	671
To	3	6.51×10^{-5}	0.9500	57	14.5×10^{-7}	0.9450	52
Si	3	5.29×10^{-5}	0.9610	74	14.3×10^{-7}	0.9460	53
Fr	3	2.08×10^{-5}	0.9895	282	2.15×10^{-7}	0.9955	671
Te	2	5.16×10^{-5}	0.9618	176	2.82×10^{-7}	0.9928	968

[a] At 95% confidence level, F statistic values: $F_{3.4} = 6.55$, $F_{2.5} = 5.79$, $F_{1.6} = 5.99$.

quite similarly regardless of temperature. This agrees with the entropy study that suggested that temperature did not affect the way H_2S adsorbed on the surface.

3.7. Model selection

Rival models were finally discriminated by examining the estimated parameters. Models for mobile adsorption (Hi, Vo) and for localized adsorption on a homogeneous surface (L1m, FG, L1d) have to be discarded because the adsorption constant K increased with temperature. Such abnormal variation was also found for models L2m and L2sm. Therefore, it can be deduced that either H_2S molecules are not present on the surface of the sulfided $CoMo/Al_2O_3$ or that H_2S molecules adsorb on more than two types of sites.

The latter hypothesis was verified by examining the multi-site models. The generalized GL model and the two Freundlich models exhibited decreasing K values with temperature; the Si, To, and Te models were thus not adequate according to this criterion. Interestingly, the exponent n in the GL equation was found to be

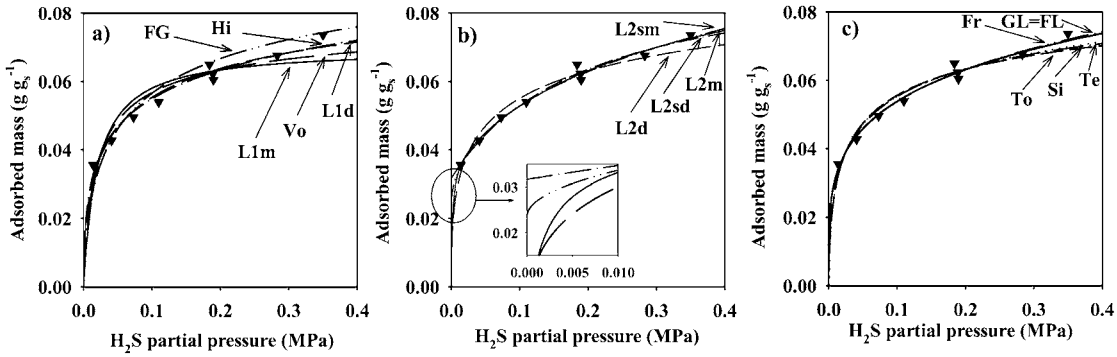

Fig. 6. H_2S adsorption isotherm at 313 K on the sulfided $CoMo/Al_2O_3$ catalyst: (a) mobile adsorption vs. localized single-site adsorption models; (b) Langmuir two-site adsorption models; and (c) multi-site adsorption models. (▼), Experimental data.

Table 5
Optimized parameters for the selected models: generalized Freundlich (FL) model and Langmuir (L2d) model featuring dissociative adsorption on alumina (A) and metallic CoMo sulfides (M) sites

Model	Parameters	Temperature (K)				
		313	353	403	493	573
FL	m_∞ (g g_s^{-1})	0.1443	0.1017	0.0824	0.0531	0.0435
	K (MPa^{-1})	0.150	0.081	0.034	0.011	0.004
	t	0.23	0.18	0.15	0.09	0.07
L2d	m_∞ (g g_s^{-1})	0.1042	0.0710	0.0509	0.0350	0.0290
	f	0.21	0.26	0.35	0.52	0.55
	K_A (MPa^{-1})	6.6	12.2	20.5	62.7	106.8
	K_M (MPa^{-1})	236	871	2932	1706	7348

1 ± 0.05, so that GL reduced to FL. With the FL (or GL) model, the slope of $\ln K$ (Table 5) versus $1/T$ gives $E = 21 \pm 2$ kJ mol^{-1}, in fair agreement with the isosteric heat Q_{st} found at the lowest temperatures (Fig. 4). On this account, the Freundlich Fr model should be discarded because the adsorption energy, $E = 3$ kJ mol^{-1} was too low. In conclusion, among all multi-site models, the generalized adsorption model FL only must be retained. Crickmore and Wojciechowski have previously showed the wide applicability of this model [22]. Thus, H_2S may possibly adsorb molecularly under a broad range of conditions on a patch-wise distribution of sites of the sulfided $CoMo/Al_2O_3$ catalyst.

However, models L2d and L2sd featuring the dissociative chemisorption of H_2S on two types of sites were as adequate as model FL (Fig. 7). Many literature studies have in fact reported that H_2S dissociates on alumina and on the metallic sulfide phases [8–10,14,15]. The estimated parameters K_A and K_M increased with temperature because of the exothermic H_2S dissociation; K_A and K_M are the products of true adsorption constants by equilibrium constants for H_2S dissociation. With model L2d, K_M was found to be about 7350 MPa^{-1} at 573 K (Table 5), in line with the adsorption constants reported on analogous $CoMo/Al_2O_3$ catalysts by Lee and Butt [32] and Leglise et al. [33] at the same temperature in kinetic studies of thiophene conversion. Thus, the magnitude of the estimated K_M using model L2d seems reasonable (Table 5). The L2sd model that supposes infinite values for K_M seems therefore over-simplified, but it was helpful for estimating the parameters of model L2d, because of the presence of several local minima in the parameter search. With model L2d, K_M was 30–140 times greater than K_A (Table 5), showing that

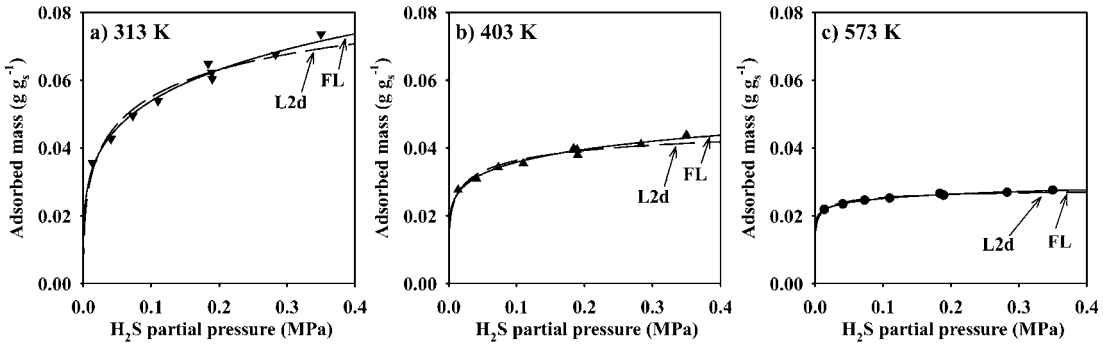

Fig. 7. H_2S adsorption isotherms on the sulfided $CoMo/Al_2O_3$ catalyst at: (a) 313 K; (b) 403 K; and (c) 573 K. Selected models: Langmuir (L2d) dissociative adsorption on two types of sites, and generalized Freundlich (FL) molecular adsorption on patch-wise distribution of sites. Filled symbols represent experimental data.

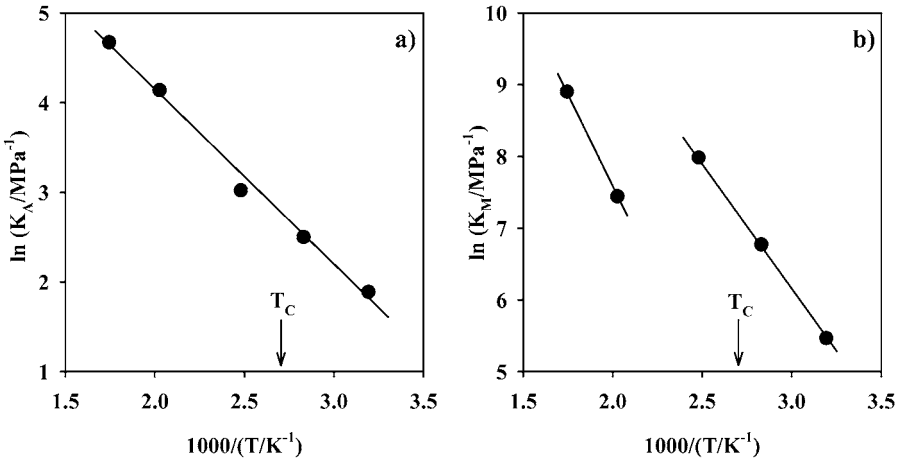

Fig. 8. Temperature dependence of Henry's adsorption constant on alumina (a) and on CoMo sulfides (b) using model L2d.

H_2S was much strongly adsorbed on CoMo sulfides than on alumina.

Fig. 8 shows the variations of K_A and K_M with temperature. A perfect linear correlation was found for the adsorption constant K_A on alumina with energy $E = -17$ kJ mol^{-1}. On the other hand, two regions were evidenced on the metallic phases: at low temperature with $E = -29$ kJ mol^{-1} and above T_c with $E = -43$ kJ mol^{-1}. This explains the observed increase of Q_{st} with temperature (Fig. 4), because the CoMo sulfides contributes more on the total adsorbed mass, as indicated by the estimated f values in Table 5. Interestingly, the results showed that the amount of H_2S adsorbed on the supported metallic phases was almost independent of temperature (Fig. 9). Hence, the decrease in H_2S uptake with increasing temperature on the $CoMo/Al_2O_3$ catalyst is essentially due to a lower contribution of the exposed alumina (Fig. 9).

In conclusion to the modelization study, two models, FL and L2d, suitably fit the experimental H_2S isotherms in the whole temperature range 313–573 K under flow and pressure conditions. H_2S molecules or species are locally adsorbed on a heterogeneous surface, in line with the thermodynamic study. The adsorption capacity of the metallic phases in the composite catalyst $CoMo/Al_2O_3$ can be evaluated using model L2d. This is clearly an advantage compared to model FL. For the purpose of catalytic application, it should be pointed out that the supported CoMo sulfides were saturated (1) at low H_2S pressure;

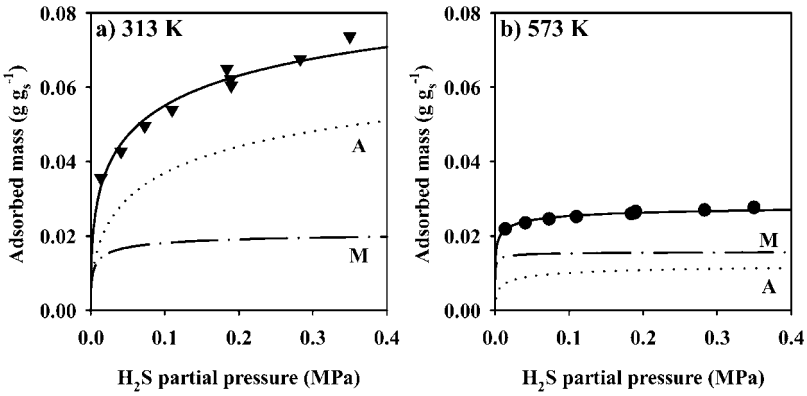

Fig. 9. Comparison of total mass adsorbed (——); and of masses adsorbed on alumina (A, ·····); and on metallic CoMo phase (M, — · —) at 313 K (a) and 573 K (b) using model L2d. Filled symbols represent experimental data.

and (2) to a rather similar extent regardless of temperature. Hence, if one wants to maximize the concentration of active sites of a hydrotreating CoMo/Al_2O_3 catalyst, the H_2S content should be kept as low as possible. Increasing the temperature should have little effect on inhibition.

4. Conclusion

Adsorption of H_2S in presence of H_2 and CH_4 on a sulfided CoMo/Al_2O_3 hydrotreating catalyst has been studied at 313–573 K under high pressure and flow conditions by thermogravimetry. The mass gain was essentially due to H_2S adsorbed on both CoMo sulfides and exposed alumina.

Study of adsorption thermodynamics shows that the isosteric heat of adsorption Q_{st} was dependent on temperature. At 313–403 K, low and constant Q_{st} values close to the heat of H_2S liquefaction were obtained. The catalyst surface appears to be homogeneous at low temperature, mainly because adsorption on the alumina fraction predominates. At 403–573 K, Q_{st} values were higher and increased linearly with the H_2S uptake, due to the predominant adsorption on CoMo sulfides. The variation in adsorption entropy indicates that H_2S adsorbs locally on the catalyst surface, and that the nature of the adsorbed H_2S species was similar regardless of temperature.

Two theoretical adsorption models were suitable to fit the experimental isotherms: the generalized Freundlich model featuring a molecular H_2S adsorption on a patch-wise distribution of sites, and the Langmuir model featuring dissociative chemisorption on both CoMo sulfides and alumina.

The amount of H_2S adsorbed on the supported CoMo sulfides was determined under conditions relevant to hydrotreatment. The modeling study indicates that CoMo sulfides were essentially saturated and to the same extent at low H_2S partial pressure regardless of temperature.

Acknowledgements

The authors thank TOTALFINAELF for funding the research. Constant support of Drs. J.L. Dubois, C. Forquy, and G. Fremy (ATOFINA) is gratefully acknowledged. One of us, M. Echard, thanks Elf-Atochem and the CNRS for the benefit of a Ph.D. grant.

References

[1] P.G. Menon, Chem. Rev. 68 (1968) 277.
[2] Y. Hori, R. Kobayashi, Ind. Eng. Chem. Fund. 12 (1973) 26.
[3] G.H. Findenegg, in: A.L. Myers, G. Belfort (Eds.), Fundamentals of Adsorption, United Eng. Trustees, New York, 1984, p. 207.
[4] J.C. Carter, in: R.P. Townsend (Ed.), The Properties and Application of Zeolites, Special Publication, Vol. 33, The Chemical Society, London, 1980 p. 76.
[5] A. Clark, in: E.M. Loebl (Ed.), The Theory of Adsorption and Catalysis, Vol. 18, Academic Press, New York, 1970.
[6] J.F. LePage et al., Applied Heterogeneous Catalysis, Design, Manufacture, Use of Solid Catalyst, Technip, Paris, 1987.
[7] H. Topsøe, B.S. Clausen, F.E. Massoth, in: J.R. Anderson, M. Boudart (Eds.), Hydrotreating Catalysis, Science and Technology, Vol. 11, Springer, Berlin, 1996.
[8] R.W. Glass, R.A. Ross, J. Phys. Chem. 77 (1973) 2576.
[9] A. Datta, R.G. Cavell, J. Phys. Chem. 89 (1985) 450.
[10] Y. Okamoto, O.H. Minoru, M. Akinori, I. Toshinobu, T. Shiichiro, J. Phys. Chem. 90 (1986) 2396.
[11] S. Kasztelan, D. Guillaume, Ind. Eng. Chem. Res. 33 (1994) 203.
[12] E. Olguin Orozco, M. Vrinat, Appl. Catal. A 170 (1998) 195.
[13] J. Leglise, L. Finot, J. van Gestel, J.C. Duchet, Stud. Surf. Sci. Catal. 127 (1999) 51.
[14] N.Y. Topsøe, H. Topsøe, J. Catal. 139 (1993) 641.
[15] O. Saur, T. Chevreau, J. Lamotte, J. Travert, J.C. Lavalley, J. Chem. Soc., Faraday Trans. I 77 (1987) 427.
[16] F. Dreisbach, R. Staudt, M. Tomalla, J.U. Keller, in: M.O. Le Van (Ed.), Proceedings of the 5th International Conference on Fundamentals of Adsorption, Kluwer Academic Press, Dordrecht, 1996, p. 259.
[17] G. De Weireld, M. Frère, R. Jadot, Meas. Sci. Technol. 10 (1999) 117.
[18] C. Eyraud, M. Escoubes, E. Robens, Tech. Ing. (1987) P1260-1.
[19] R.C. Reid, J.M. Prausnitz, B.E. Poling, The properties of gases and liquids, 4th Edition, MacGraw-Hill, New York, 1987.
[20] M.H. Simonot-Grange, J. Chim. Phys. 94 (1987) 1161.
[21] M. Jarionec, in: A.L. Myers, G. Belfort (Eds.), Fundamentals of Adsorption, United Eng. Trustees, New York, 1984, p. 239.
[22] J. Crickmore, B.W. Wojciechowski, J. Chem. Soc. Faraday Trans. I 73 (1977) 1216.
[23] J. Tòth, in: A.L. Myers, G. Belfort (Eds.), Fundamentals of Adsorption, United Eng. Trustees, New York, 1984, p. 657.
[24] M. Echard, J. Leglise, Catal. Lett. 72 (2001) 83.
[25] O. Talu, I. Zwiebel, A.I.Ch.E. J. 32 (1986) 1263.

[26] N. Tokunaga, H. Oshiyama, T. Nitta, T. Katayama, J. Chem. Eng. Jpn. 21 (1988) 431.
[27] C. Gachet, Y. Trambouze, J. Chim. Phys. 67 (1970) 2072.
[28] Handbook of Chemistry and Physics, 73rd Edition, CRC Press, Boca Raton, 1992.
[29] L.A. Garden, G.L. Kington, Proc. R. Soc. Series A 234 (1956) 24.
[30] C.J. Wright, C. Sampson, D. Fraser, R.B. Moyes, P.B. Wells, J. Chem. Soc. Farad. I 76 (1980) 1585.
[31] R.K. Agarwal, K.A.G. Amankwah, J.A. Schwarz, Carbon 28 (1990) 169.
[32] H.C. Lee, J.B. Butt, J. Catal. 49 (1977) 320.
[33] J. Leglise, J. van Gestel, J.C. Duchet, Am. Chem. Soc. Div. Petr. Prep. 39 (1994) 533.